Thermal properties of halogen-ethane glassy crystals: Effects of orientational disorder and the role of internal molecular degrees of freedom

G. A. Vdovichenko,[1] A. I. Krivchikov,[1] O. A. Korolyuk,[1] J. Ll. Tamarit,[2,a)] L. C. Pardo,[2] M. Rovira-Esteva,[2] F. J. Bermejo,[3] M. Hassaine,[4] and M. A. Ramos[4]

[1]*B. Verkin Institute for Low Temperature Physics and Engineering of NAS Ukraine, 47 Lenin Ave., 61103 Kharkov, Ukraine*

[2]*Grup de Caracterització de Materials, Departament de Física i Enginyeria Nuclear, ETSEIB, Universitat Politècnica de Catalunya, Diagonal 647, 08028 Barcelona, Catalonia, Spain*

[3]*Instituto de Estructura de la Materia, CSIC, Consejo Superior de Investigaciones Cientificas, Serrano 123, 28006 Madrid, Spain*

[4]*Laboratorio de Bajas Temperaturas, Departamento de Física de la Materia Condensada, Condensed Matter Physics Center (IFIMAC) and Instituto Nicolás Cabrera, Universidad Autónoma de Madrid, Francisco Tomás y Valiente 7, 28049 Madrid, Spain*

(Received 12 June 2015; accepted 13 August 2015; published online 27 August 2015)

The thermal conductivity, specific heat, and specific volume of the orientational glass former 1,1,2-trichloro-1,2,2-trifluoroethane (CCl_2F–$CClF_2$, F-113) have been measured under equilibrium pressure within the low-temperature range, showing thermodynamic anomalies at ca. 120, 72, and 20 K. The results are discussed together with those pertaining to the structurally related 1,1,2,2-tetrachloro-1,2-difluoroethane (CCl_2F–CCl_2F, F-112), which also shows anomalies at 130, 90, and 60 K. The rich phase behavior of these compounds can be accounted for by the interplay between several of their degrees of freedom. The arrest of the degrees of freedom corresponding to the internal molecular rotation, responsible for the existence of two energetically distinct isomers, and the overall molecular orientation, source of the characteristic orientational disorder of plastic phases, can explain the anomalies at higher and intermediate temperatures, respectively. The soft-potential model has been used as the framework to describe the thermal properties at low temperatures. We show that the low-temperature anomaly of the compounds corresponds to a secondary relaxation, which can be associated with the appearance of Umklapp processes, i.e., anharmonic phonon-phonon scattering, that dominate thermal transport in that temperature range. © *2015 AIP Publishing LLC.* [http://dx.doi.org/10.1063/1.4929530]

I. INTRODUCTION

The term *plastic* or *rotator-phase crystal* denotes a crystalline arrangement of weakly interacting bodies, often of molecular nature, which albeit showing translational long-range order, exhibit dynamical orientational disorder, namely, the bodies forming the plastic crystal maintain their overall position anchored to the lattice points, but experience thermal reorientation fluctuations.[1,2] The existence of these degrees of freedom has long been known to be the reason for the mechanical softness and low melting enthalpy of plastic crystals.

When cooled down below low-enough temperatures, some plastic crystals show specific heat and dynamic anomalies characteristic of glass transitions.[3] At the temperature where such glass transitions take place, the dynamical orientational disorder of the plastic crystal becomes arrested and a quasi-static orientationally disordered crystal is obtained. This kind of arrested crystal is known as *orientational glass* or *glassy crystal*.[3,4]

Additionally, other degrees of freedom, such as internal molecular rotations, can also be thermally activated within the plastic crystalline or glassy crystalline phases.

The halogen-ethane derivatives ($C_2X_{6-n}Y_n$, with X, Y = H, Cl, F, Br) are well known examples of compounds exhibiting this kind of solid phases. The relevance of studying such crystals stems from the fact that they are among the simplest model systems where the effects of an internal molecular degree of freedom, such as the rotation about the C–C chemical bond, can be investigated. The flexibility of this bond allows one side of the molecule to rotate with respect to the other, which leads in many compounds to two energetically distinct rotamers or conformational isomers. Although the energy barrier between the conformers is large, their energy difference is much smaller, and is expected to significantly decrease within the condensed phases, since such lowest frequency internal modes strongly couple to the lattice motions. In addition, the coexistence of two conformers has been observed in the vapor, liquid, and solid states.[5–11]

The interplay of the many degrees of freedom within these systems hinders the nucleation of their stable phase, and thus promotes the emergence of metastable phases for a wide temperature range. Early studies by Kolesov *et al.*

a)Electronic mail: josep.lluis.tamarit@upc.edu

on some halogen ethanes, namely, 1,1,2,2-tetrachloro-1,2-difluoroethane ($CCl_2F–CCl_2F$, hereafter F-112), 1,1,2-trichloro-1,2,2-trifluoroethane ($CCl_2F–CClF_2$, hereafter F-113), and 1,2-dichloro-1,1,2,2-tetrafluoroethane ($CClF_2–CClF_2$), already pointed out the difficulty to obtain their low-temperature fully ordered crystal phases.[12,13] In fact, the molecules of this family of compounds are so easily arrested in disordered glassy crystalline states that F-112 is the most fragile plastic crystal known so far (note that *fragility* refers here to the measure of how abruptly it changes the orientational dynamics with the temperature variations).[14] Several authors have linked the existence of the F-112 internal molecular degree of freedom to this outstanding facility to supercool its plastic crystalline phase.[14–19]

Halogen-ethane derivatives have been thoroughly characterized macroscopically (heat capacity, thermodynamic magnitudes, phase transitions, etc.) and microscopically (molecular dynamics, crystallographic structure, relaxation dynamics, molecular structure, etc.) seeking to find a relation between its physical properties and its intermolecular interactions, as well as its intramolecular features, which can influence both the short- and the long-range order.[14–22]

F-112 and F-113 are archetypal examples in which a mixture of conformers is present, and for which a complicated sequence of calorimetric transitions appears. Figure 1 shows the two F-112 conformers, gauche and trans, and the two F-113 conformers, C_1 and C_s.

For F-112, early specific heat (C_p) measurements revealed three thermal anomalies. Namely, a step-like feature appearing about 130 K attributed to the arrest of the conformational degree of freedom, a pronounced jump in C_p at 90 K due to the orientational glass transition, and an additional anomaly around 60 K.[16] Above 130 K, molecules sitting in the body-centered cubic (bcc) plastic crystal experience fluctuations in their overall orientation, as well as in their internal rotation. Below 130 K, the conformational disorder of the molecules is assumed to become frozen and they are stuck with the conformation they had at the onset of the conformational arrest, but they can still reorient as a whole, and experience torsional low-amplitude oscillations about the *C–C* bond.

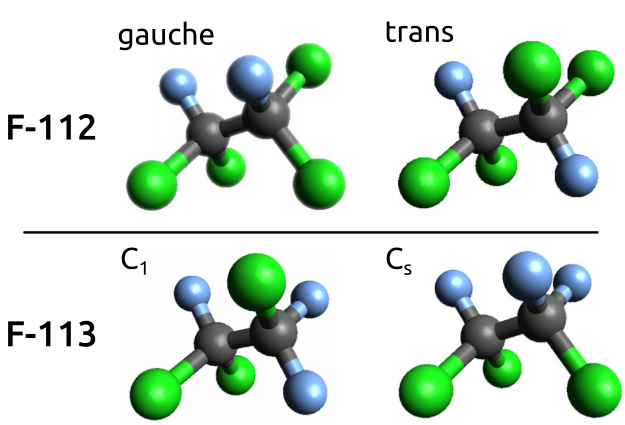

FIG. 1. Scheme of the two energetically distinct molecular rotamers of 1,1,2,2-tetrachloro-1,2-difluoroethane (F-112), gauche and trans, and of 1,1,2-trichloro-1,2,2-trifluoroethane (F-113), C_1 and C_s. Atom color codes are green for Cl, blue for F, and grey for C.

However, at $T_g \approx 90$ K the primary glass transition takes place and the orientational disorder also becomes arrested. The anomaly at 60 K was attributed to a secondary relaxation, but it still has an unclear physical origin. While other plastic crystals exhibit no or only weak secondary relaxations, F-112's strong secondary relaxation is still a matter of controversy.

Furthermore, an unusually wide thermal conductivity plateau for F-112's glassy crystal was recently reported by some of the authors of this work. This plateau extends from 10 K up to 70–80 K, almost up to the glass transition temperature, and was suggested to be induced by a resonant scattering of phonons caused by simple oscillators.[17]

It should also be mentioned that for F-112, only a scarce 2%-3% of a more stable low-temperature crystalline phase was obtained after annealing the glassy crystalline phase for 50 days.[16]

In general, trans conformers are energetically favored over gauche conformers in the vapor state of most substances. However, the opposite behavior where the gauche conformer is more stable than the trans conformer, known as *gauche effect*, has been reported for a few compounds, in particular for some halogen-ethane derivatives.[23–26] Rovira-Esteva *et al.* have recently shown that this is the case for F-112 as well, and that its gauche rotational isomer is in fact more stable than the trans one, with the gauche conformer representing about 68% of the molecular population in the liquid state.[15] The energy barrier and energy difference between the two conformers were experimentally determined in this compound using NMR, Raman and far infrared spectroscopy, and specific heat measurements, which yielded, respectively, 29–40 kJ mol^{-1} and 0.51–0.79 kJ mol^{-1}.[15,16,27–29]

F-113 has been much less studied. Its molecule shows two geometrical conformations related to each other by a rotation of about 120° around the C–C single bond, as shown in Figure 1. One of the conformers, characterized by a trans position of two C–Cl and C–F bonds, has a C_1 point/group symmetry while the other one, characterized by a gauche position of all the C–Cl and C–F bonds, shows C_s symmetry. The energy barrier between both conformers has recently been determined within the gas phase and is of the order 24 – 30 kJ mol^{-1} depending upon the conformer, while their energy difference is about 1.6 kJ mol^{-1}.[30] Infrared and electron diffraction studies of F-113 have shown a mixture of both C_1 and C_s isomers for the plastic crystalline, liquid, and vapor phases studied across the temperature range 173–353 K, with the C_1 conformer being more stable than the C_s conformer.[31–33]

Kolesov *et al.* measured the specific heat from 6 K up to 300 K for the various stable solid and liquid phases and reported the formation of a plastic crystalline phase below the melting temperature $T_m = 238$ K.[12,13] They suggested that at the lower temperatures of the plastic crystalline phase, the ratio between the C_1 and C_s conformers must be frozen. This plastic crystalline phase can be easily supercooled and undergoes a glass transition into a glassy crystalline phase at $T_g \approx 70$ K. Moreover, they were also able to obtain a more stable low-temperature crystalline phase than the glassy crystal by gradual cooling of the plastic crystal and then annealing the sample for 10–14 h. However, this low-temperature crystalline phase still has a significant amount of residual entropy, which

suggests a certain degree of arrested disorder. On heating, this low-temperature crystalline phase transforms at 82.5 K into the plastic crystalline phase.

The purpose of the present article is to report on new measurements of the thermal properties of F-113 and to compare them to measurements of F-112, which have been already partially reported. The interest of such an exercise stems from the extremely different behavior exhibited by the thermal and transport properties of these two chemically close materials. The research reported here has focused on the effects of the thermally activated degrees of freedom of both materials on their thermal and transport properties, such as the thermal conductivity, specific heat, and specific volume.

II. EXPERIMENTAL DETAILS

We have used 1,2,2-trichloro-1,1,2-trifluoroethane (CCl_2F–$CClF_2$, F-113) purchased from Aldrich, with purity >99.7%, and 1,1,2,2-tetrachloro-1,2-difluoroethane (CCl_2F–CCl_2F, F-112) from ABCR GmbH & Co. KG, with purity >99%.

Structural changes across the studied temperature range were monitored using the high-intensity neutron diffractometer D1b at the Institute Laue-Langevin (ILL, Grenoble) with a wavelength of $\lambda = 2.52$ Å. The position-sensitive detector had a step size of 0.2° and was setup to cover a 2θ-range from 20° to 100°.

The samples were measured through several temperature cycles with different heating and cooling rates. Slight differences were observed depending upon the thermal history, however, these differences are irrelevant for the present study. Hence, the measurements shown here correspond to a slow heating rate of 0.5 K/min within the temperature range 3–260 K, after previously having cooled down the sample at 1 K/min.

Specific heat measurements were carried out using a versatile calorimetric system especially designed for glass-forming liquids, and described in detail elsewhere.[34] In brief, the sample is enclosed in a copper cell with very thin walls, which has a resistive heating element and a carbon ceramic sensor (CCS) attached. The CCS sensor is used as thermometer and is calibrated from 1.4 K to room temperature. The cell is then inserted in a glass cryostat which either employs He or N_2 liquids as cryogens, depending on the temperature range of interest. The experimental setup includes a double chamber insert to allow an independent thermal control, and operates under a vacuum environment reaching a range of 10^{-7}–10^{-8} mbars.

Clean syringes were always employed to fill the calorimetric cell with the liquid samples, which was then immediately sealed to avoid contamination with air moisture. The mass of the F-112 sample was 0.426 g and that of the F-113 sample was 0.536 g, while the mass of the empty copper cell was 1.709 g.

Two different calorimetric methods have been employed in this work. At lower temperatures (1.7–20 K), we followed the thermal relaxation method, either within the standard version or within an alternative procedure devised for materials showing longer relaxation times between cell and thermal sink.[34] For higher temperatures (20–260 K), we followed a quasi-adiabatic continuous method previously implemented, which has been successfully employed in glass-forming liquids above liquid-N_2 temperatures and in solids above liquid-He temperatures.[34–36] In this quasi-adiabatic continuous method, the heat capacity is determined from a dual (cooling + heating) experiment, typically using rates around ±1 K/min, being the distinctive behavior of the sample cell between both runs which provides the measurement of its heat capacity.[34,36] The heat capacity of the empty cell is measured in a different run to subtract the addenda contribution.

The thermal conductivity of the plastic crystalline and glassy crystalline phases of F-113 was measured under equilibrium vapor pressure in an experimental setup that uses the steady-state potentiometric method.[37,38] The glassy state was prepared by cooling (above 1 K/min) the plastic crystalline phase through the glass transition region. The thermal conductivity was measured with gradually decreasing temperature within the range 2–125 K, for the corresponding phase below or above T_g, following the same experimental procedure previously used in F-112, as well as in other glassy crystals and structural glasses.[17,39–41]

III. RESULTS

Neutron diffraction experiments allow to determine the crystalline structures of F-113 and F-112 as a function of the temperature. Both the plastic and the glassy crystalline phases of F-113 display a bcc structure, as was also previously reported for F-112.[19] Figure 2(a) shows a few of the diffractograms obtained for F-113 and F-112, where the shift in the position of the diffraction peaks with temperature is clearly apparent. Fits to these neutron scattering measurements allow to obtain the characteristic parameters of the sample structure. Figure 2(b) shows the variation of the bcc lattice parameter a as a function of the temperature for both compounds. Such measurements reveal a series of signatures for F-112 at temperatures that correspond to those previously reported. Several unreported anomalies can also be observed for F-113, in these measurements even more pronounced than those of F-112.

At $T_g \approx 72$ K, the primary glass transition of the F-113 plastic crystal to a glassy crystal takes place, where the overall molecular reorientation becomes arrested. The counterpart in F-112 for such a transition occurs at about 90 K. In both cases, the glass transition is evidenced by a change in the thermal expansivity, a thermodynamic signature.

F-113 also displays a manifest variation in the thermal expansivity around 120 K. Above 120 K, the molecules in the bcc lattice are able to experience overall, large-angle reorientation fluctuations and, possibly, transform from the C_1 conformer into the C_s, and vice versa. Within such a view, below 120 K molecular motions are restricted to reorientation and torsional small-angle fluctuations. This hypothesis is supported by the fact that the lattice parameter features displayed by F-113 qualitatively resemble those of F-112, for which a conformational arrest was previously suggested by several authors to explain its anomaly at 130 K,[15,16] and is also

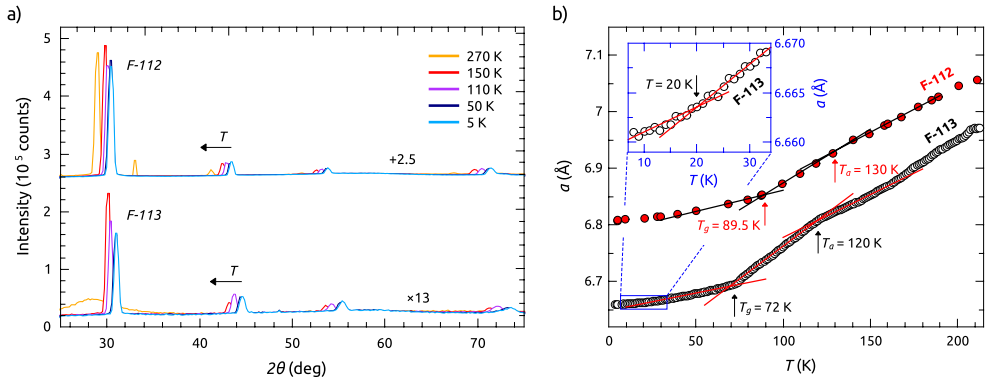

FIG. 2. (a) A few neutron diffractograms of F-113 and F-112 at the phases of interest. As temperature increases, peak positions shift to smaller angular values due to dilatation effects in the structure. However, between 5 K and 50 K this effect is too small to be clearly apparent in this figure. The intensity from the two experiments has been rescaled and shifted for a better comparison. (b) Variation of the bcc lattice parameter a as a function of temperature for F-113 (empty circles) and F-112 (full red circles). Several anomalies, qualitatively mimicking those of F-112, can be observed for F-113. Temperatures at which the different thermal anomalies discussed in the text appear have been marked by arrows. The possible relaxational feature of F-112 at 60 K cannot be studied in these measurements for lack of data. The inset shows a magnification of the lowest temperature range for F-113 to show its behavior around the thermal feature at 20 K.

supported by Kolesov *et al.*'s suggestion that the ratio between the C_1 and C_s conformers is frozen at the lower temperature range of the F-113 plastic crystal.[13]

Finally, for F-113 the dependence of the lattice parameter with temperature also seems to change slightly at ca. 20 K. For F-112, a specific heat anomaly within the lowest temperature range, which was attributed to a secondary relaxation, was found at 60 K.[16] Unfortunately, this possible relaxational feature cannot be addressed in the F-112 lattice parameter measurements reported here since available data are not detailed enough for the purpose.

Additionally, the zero-temperature limits of the mass density $\rho(0)$ of F-113 and F-112 have been obtained from the lattice parameter a, in order to determine their corresponding Debye temperatures θ_D, which will be needed for the soft potential model (SPM) calculations. Since there are two molecules per unit cell in the bcc lattice, the molecular volume is simply $a^3/2$. The zero-temperature mass density $\rho(0)$ for the glassy crystal of each compound can be determined by extrapolating the lattice parameter to 0 K. For F-112, $a(0)$ = 6.81 Å and hence $\rho(0)$ = 2.14 g/cm^3, in good agreement with previously published values,[42] and for F-113, $a(0)$ = 6.66 Å and hence $\rho(0)$ = 2.11 g/cm^3. The zero-mass densities $\rho(0)$, Debye temperatures θ_D, and other basic thermodynamic data are summarized in Table I.

Our F-113 specific heat measurements for all temperature ranges are shown together in Figure 3. The peak corresponding to the melting transition can be found around T_m = 235 K. The very small specific heat difference observed between the liquid and the crystalline phases at the melting temperature should be stressed. Such small difference is characteristic of materials having a high degree of disorder, such as plastic crystals.

As can be seen, specific heat measurements also exhibit signatures that correlate with the anomalies found in F-113's lattice parameter. Its main glass transition (between the plastic and the glassy crystalline phases) is observed at T_g = 72 K (measured at ~1 K/min), with a discontinuity in the specific heat of $\Delta C_p = 51.4 \pm 1.6$ J K^{-1}mol^{-1}. The specific heat discontinuity has been calculated by extrapolating the baselines of the glassy crystal (below T_g) and the plastic crystal (above T_g). Interestingly, the heat capacity curve of the glassy crystal monotonically increases with temperature, clearly surpassing the Dulong-Petit limit for a rigid molecule, which suggests a larger number of degrees of freedom being thermally activated.

The relaxational feature observed in the heat-capacity at 120 K for F-113 (see inset in Figure 3) amounts to $\Delta C_p = 1.3 \pm 0.4$ J K^{-1} mol^{-1}, which is not far from that measured for F-112 at 130 K, $\Delta C_p = 1.1 \pm 0.2$ J K^{-1} mol^{-1}.[16] Such similar values suggest that these two features could be ascribed

TABLE I. Some basic thermodynamic parameters for F-112 and F-113: molecular mass (M), orientational glass transition temperature between plastic and glassy crystalline phases (T_g), specific heat discontinuity at T_g (ΔC_p), temperature of the thermal anomaly ascribed to the conformational arrest of the molecule (T_a), temperature of the boson peak in C_p/T^3 (T_{BP}), zero-temperature mass density from neutron-diffraction data ($\rho(0)$), Debye sound velocity (v_D), and Debye temperature (Θ_D). The values estimated from the soft potential model fit to the specific heat C_p measurements are given in parentheses.

Glassy crystal	M (g mol^{-1})	T_g (K)	ΔC_p (J mol^{-1} K^{-1})	T_a (K)	T_{BP} (K)	$\rho(0)$ (kg m^{-3})	v_D (m s^{-1})	Θ_D (K)
F-112	203.83	89.5[a]/90[b,c]	53.8[a,c]	130[b]	4.5[a]	2140[a]	1380[d]	76[d]
F-113	187.38	72[a]	51.4[a]	120[a]	5.0[a]	2110[a]	(1420)[a]	(80)[a]

[a]This work.
[b]Reference 17.
[c]Reference 16.
[d]Reference 42.

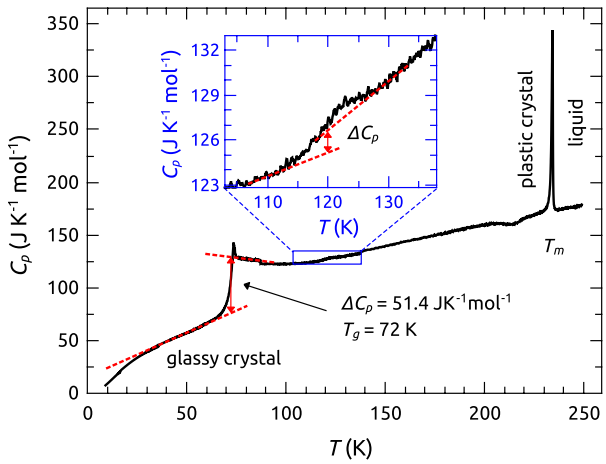

FIG. 3. Specific heat of F-113 as a function of the temperature, where features corresponding to phase transitions and anomalies studied in this work are observed. At the higher temperature range, the melting peak indicates the transition between the liquid and plastic crystalline phases, and at 72 K the specific heat discontinuity reveals the glass transition between the plastic and glassy crystalline phases. The inset shows a magnification of the specific heat anomaly at 120 K, ascribed to the conformational arrest of the proportion between rotamers C_1 and C_s.

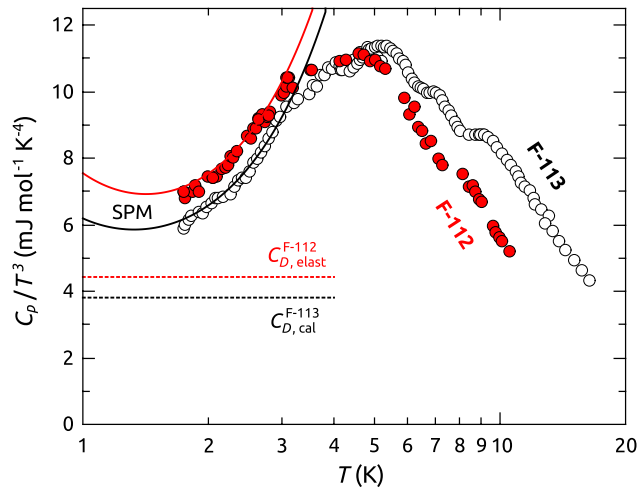

FIG. 4. Low-temperature reduced specific heat C_p/T^3 for F-112 (full red circles) and F-113 (empty circles), exhibiting the boson peak at 4.5 K and 5 K, respectively. Fits to the lower temperature range, following the soft potential model (SPM), are shown by solid lines. The Debye coefficients C_D, obtained from elasto-acoustic measurements for F-112 and from the SPM fit for F-113 are indicated by dotted lines.

to the same physical phenomenon for both compounds. Since the thermal anomaly in F-112 has been previously attributed to the arrest of the molecular transformations between trans and gauche conformers, this supports the idea that F-113's anomaly observed at 120 K could also arise from the arrest of the transformations between the C_1 and C_s conformers.

Similar specific heat measurements conducted in F-112 (not shown here) presented a glass-like transition at T_g = 89.5 K with a $\Delta C_p = 53.8 \pm 1.5$ J mol^{-1} K^{-1}, which corresponds to the orientational glass transition, in very good agreement with previous data from other authors.[13,16]

The so-called *boson peak* can be observed in Debye-reduced specific heat C_p/T^3 measurements, and is an almost universal feature of glasses,[43] including glassy crystals.[44] Figure 4 shows the reduced specific heat at low temperature for both compounds. F-113 has its boson peak maximum at T_{BP} = 5.0 K, while F-112 has the maximum at T_{BP} = 4.5 K.

Thermal conductivity $\kappa(T)$ as a function of the temperature is shown in Figure 5 for the glassy and plastic crystalline phases of F-113. For the sake of comparison, previously published values are also shown for the glassy and plastic crystalline phases of F-112.[17] It can be seen that the thermal conductivity $\kappa(T)$ displays for both compounds the typical behavior of glasses at low temperatures, and that of crystals at higher temperatures. More specifically, for F-113 the thermal conductivity increases with increasing temperature up to a maximum around 4.5 K. Beyond this point, a smeared plateau follows, which extends over a relatively narrow temperature range, approximately from 5 to 20 K. At about 20 K, $\kappa(T)$ shows a kink, after which it strongly decreases with temperature until essentially the main glass transition $T_g \approx 72$ K (corresponding to the transition between the plastic and glassy crystalline phases).

For F-112, the same qualitative behavior was previously reported.[17] The quantitative differences concern mainly the extension of the plateau, which persists towards the kink appearing in F-112 at about 60 K, and the significantly smaller values of $\kappa(T)$ found at low temperatures for the glassy crystal of F-112 with respect to F-113.

On the basis of the simple phonon-gas model, the thermal conductivity is related to the phonon specific heat C_{ph}, the averaged sound velocity v_s, and the phonon mean free path l_{ph}, through the following relationship:

$$\kappa(T) = \frac{1}{3} C_{ph}\, v_s\, l_{ph}. \tag{1}$$

Taking into account the similarity of the phonon specific heat C_{ph} and the sound velocity v_s between F-112 and F-113 (see Table I), it follows that similar values should be expected for their low-temperature thermal conductivity. However, it

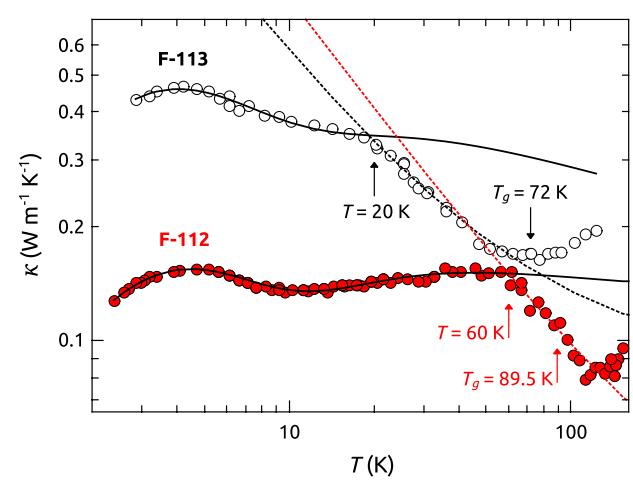

FIG. 5. Thermal conductivity as a function of temperature (in log-log scale) for the glassy and plastic crystalline phases of F-113 (empty circles) and F-112 (full red circles). Continuous lines account for the $\kappa_{ph}(T)$ contribution (see Equation (3)). Dotted lines account for the $\kappa(T) = A/T + B$ contribution (see Equation (7)) between the low temperature anomaly and the main glass transition temperature (range from 20 K to 72 K for F-113, and from 60 K to 89.5 K for F-112).

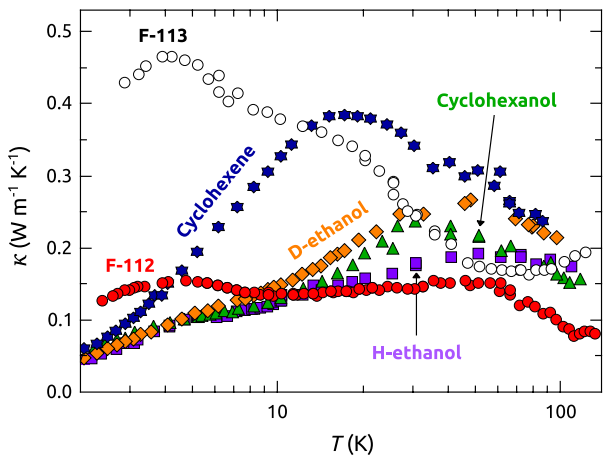

FIG. 6. Thermal conductivity as a function of temperature (in semi-log scale) of F-113 (empty circles), and comparison of its low-temperature behavior with that of several glassy crystals previously reported: F-112[17] (red circles), cyclohexanol[39] (green triangles), H-ethanol[45] (violet squares), D-ethanol[40] (orange diamonds), and cyclohexene[46] (blue stars). F-113 shows remarkably high values of the thermal conductivity at low temperatures.

can be seen in Figure 5 that this is in strong contrast with experimental results, with F-113 exhibiting much larger values than F-112. Moreover, when comparing the thermal conductivity at low temperatures for several glassy crystals (see Figure 6), it becomes clear that the unusually high values found in F-113 deserve special attention.

IV. DISCUSSION

At low temperatures, both specific heat and thermal conductivity of glasses or amorphous solids exhibit an astonishing universal behavior.[43,47] Below 1–2 K, the specific heat of glasses depends quasilinearly on temperature, $C_p \propto T^{1+\delta}$, and the thermal conductivity almost quadratically, $\kappa \propto T^{2-\delta}$, in contrast with the cubic dependence successfully predicted in ordered crystals for both properties by Debye's theory.

In addition, the thermal behavior of glasses above ~2 K and the corresponding low-frequency vibrational density of states $g(\omega)$ around 1 THz are dominated by another universal feature of glasses: the boson peak. This peak arises from a significant excess of the density of states $g(\omega)$ over Debye's prediction $g(\omega) \propto \omega^2$. Such "glassy excess" in low-frequency excitations translates into a broad peak in $g(\omega)/\omega^2$, which in turn produces a broad maximum in the reduced specific heat C_p/T^3, typically observed in glasses at 3–10 K.[43] The scattering of thermal acoustic phonons by those additional low-frequency excitations seems to be the cause of the plateau in the thermal conductivity also universally observed for any glass within that same temperature range.[43,47–50] Interestingly, glassy crystals have been found to exhibit the very same universal glassy behavior as truly amorphous solids.[17,44,51]

Thermal and acoustic properties of amorphous solids below 1–2 K were soon successfully accounted for by the tunneling model, which postulates a random distribution of independent tunneling states or two-level systems (TLS) from asymmetric energy barriers produced by atomic disorder.[43] However, thermal properties of glasses above 1 K and the corresponding low-frequency vibrational spectrum featuring the boson peak are still much more controversial.

The soft potential model (SPM) has been used to explain the behavior at low temperatures of the two compounds. This phenomenological model can be regarded as an extension of the tunneling model and postulates the coexistence in glasses of acoustic phonons with quasilocalized low-frequency soft modes[48–50,52] (for a review of the original model, see Ref. 52). Such low-frequency modes are described by a random distribution of quartic potentials, either single-well (quasiharmonic vibrations) or double-well (anharmonic two-level system) potentials. The central potential-energy parameter W of the SPM marks indeed the crossover from the region dominated by the two-level systems at the lowest temperatures, to another region where the dominant excitations are quasiharmonic soft modes. These constitute the lower frequency tail of the boson peak and the thermal conductivity plateau. The density of vibrational states in this region dominated by soft modes is $g(\omega) \propto \omega^4$ in the lower frequency limit.[49,50]

Although there are other models or theories about the low-temperature properties of disordered matter, we believe that the SPM is the only one which allows us to concurrently and quantitatively discuss thermal conductivity and specific heat data of glassy systems. Despite this, we have measured the specific heat and the thermal conductivity only above 1.7 K and 2 K, respectively, and hence a very accurate determination of the SPM parameters is not guaranteed due to this basic SPM being strictly valid well below the boson-peak maximum, we consider it, however, a useful method to assess the observed low-temperature glassy excitations and the acoustic phonon contribution, as well as to check the consistency of the SPM.

In its simplest version, the SPM coincides with the tunneling model below 1–2 K, predicting a quasilinear temperature dependence $C_{\mathrm{TLS}}T$ in the specific heat C_p, and a quadratic term in the thermal conductivity $\kappa(T)$. For temperatures roughly above $W/(2k_B)$, the specific heat is dominated by the $C_{\mathrm{sm}}T^5$ term arising from the soft modes, apart from the standard Debye contribution C_DT^3, and the thermal conductivity becomes roughly constant (the plateau range).[49,50]

Therefore, this model conveniently allows to describe the specific heat of glasses below the boson peak maximum in C_p/T^3 (including glassy crystals) through a simple equation with three contributions,[53]

$$C_p = C_{\mathrm{TLS}}T + C_DT^3 + C_{\mathrm{sm}}T^5. \tag{2}$$

In the case of F-112, previously reported values for its longitudinal sound velocity down to low temperatures, together with measurements of the elastic-stiffness coefficients below room temperature, allow to determine its Debye contribution coefficient C_D.[42,54] The generalized Cauchy equation $v_L^2(T) = A + 3v_T^2(T)$, which links longitudinal v_L and transverse v_T sound velocities, allows to determine the Debye-averaged sound velocity v_D in the zero-temperature limit.[54] Since the Debye contribution C_DT^3 is calculated in the low-temperature limit from elasto-acoustic measurements for F-112, this means that only two parameters are needed for the SPM fit at low temperature: C_{TLS} and C_{sm}.[41] The C_D coefficient is determined first and, then, the two free parameters C_{TLS}

TABLE II. Parameters of the soft potential model obtained from the fits to specific heat and thermal conductivity measurements. The C_D value for F-112 (in parentheses) has been determined from elasto-acoustic measurements.

Glassy crystal	W/k_B (K)	$\bar{C}$ ($\times 10^{-4}$)	C_{TLS} (mJ mol^{-1} K^{-2})	C_D (mJ mol^{-1} K^{-4})	C_{sm} (mJ mol^{-1} K^{-6})
F-112	2.5	2.8	2.50	(4.43)	0.621
F-113	2.4	0.84	1.80	3.81	0.581

and C_{sm} are obtained by a straight-linear fit well below the boson peak of $(C_p - C_D T^3)/T$ versus T^4, as done by Hassaine *et al.*[41]

To the best of our knowledge, there are no sound-velocity values reported for the glassy crystal in the case of F-113, hence, the Debye coefficient C_D cannot be determined from elasto-acoustic measurements and all three heat capacity coefficients must be determined from the fit. Thus, we have estimated C_D and hence v_D calorimetrically from a fit of the lower temperature of the specific heat C_p measurements using the SPM model. A parabolic fit of C_p/T versus T^2 at low temperatures provides the three calorimetric coefficients for the basic SPM equation, including the Debye coefficient C_D.[53] The SPM fits, together with the Debye contributions of F-112 and F-113 ($C_{D,\,\mathrm{elast}}^{\mathrm{F112}}$ and $C_{D,\,\mathrm{cal}}^{\mathrm{F113}}$, respectively), are shown in Figure 4.

The central potential-energy parameter W of the SPM can be determined directly from the relationship $W/k_B \approx 1.8\,T_{\min}$, where $T_{\min} = (C_{TLS}/C_{sm})^{1/4}$. Within the SPM, C_{TLS} and C_{sm} are interrelated because both are directly proportional to the density of quasilocalized soft modes. All these values are given in Table II.

On the other hand, the thermal conductivity has been studied within the framework of the SPM, employing the standard expression for the density of states of sound modes obtained in the Debye approximation,[48–50,55]

$$\kappa_{ph}(T) = \frac{k_B^4 T^3}{2\pi^2\hbar^3 v_s}\int_0^{\Theta_D/T} \tau_R(x)\,\frac{x^4 e^x}{(1-e^x)^2}dx, \qquad (3)$$

where $x = \hbar\omega/k_B T$, v_s is the speed of sound averaged over longitudinal and transverse polarizations, Θ_D is the Debye temperature, and $\tau_R^{-1}(\omega)$ is the averaged phonon relaxation rate directly associated to the phonon mean free path.

In the SPM, the relaxation rate $\tau_R^{-1}(x)$ is driven by three different contributions, which are the resonant scattering of sound waves by tunneling (τ_{TLS}^{-1}) or soft quasilocalized vibrations (τ_{vibr}^{-1}), and the classical relaxational processes in the asymmetric double-well potentials (τ_{class}^{-1}). According to the Matthiessen rule

$$\tau_R^{-1}(\omega) = \tau_{TLS}^{-1} + \tau_{vibr}^{-1} + \tau_{class}^{-1}. \qquad (4)$$

If the three contributions to the SPM relaxation rate are written explicitly, we obtain the following expression:[48–50]

$$\tau_R^{-1} = \bar{C}\pi\omega\tanh\left(\frac{\hbar\omega}{2k_B T}\right) + \ln^{-1/4}\left(\frac{1}{\omega\tau_0}\right)\bar{C}\pi\omega\left(\frac{k_B T}{W}\right)^{3/4} + \frac{\bar{C}\pi\omega}{8}\left(\frac{\hbar\omega}{W}\right)^3. \qquad (5)$$

The relevant parameters in this equation are thus $\bar{C}$, a dimensionless constant accounting for the coupling strength between a sound wave and the soft quasilocalized mode, W, the characteristic energy of the quartic term entering the potential of the SPM, and τ_0^{-1}, an attempt frequency of the order of 10^{-13} s. W scales the elementary excitations in the quasiharmonic soft potential in such a way that it characterizes the crossover between two regimes: one dominated by phonon scattering by two-level systems, when $\hbar\omega \ll W$, and another for which quasilocalized low-energy vibrational modes emerge as the main resonant scattering centers for sound waves, when $\hbar\omega \geq W$. It should be noted that in Equation (5) only $\bar{C}$ and W are relevant fitting parameters, because the logarithmic factor is approximately a constant: $\ln^{-1/4}(1/\omega\tau_0) \approx 0.7$.

The phonon relaxation rate from Equation (5) can be used in Equation (3) to perform the fit. The parameters obtained from the SPM fit to experimental data for F-113 and F-112 are gathered in Table II, both for specific heat and thermal conductivity measurements at low temperatures. Although the absolute accuracy of these SPM parameters should be taken with caution for the reasons mentioned above, it must be emphasized that a consistent common W value was obtained from both C_p and κ fits. It is also worth mentioning the close similarity of the values obtained for the W for both glassy crystals. This potential energy accounts for the crossover between the regime in which phonon scattering is due to tunneling two-level systems and that in which it is governed by quasilocalized low-frequency vibrations. Hence, according to the SPM, the temperature at which the plateau starts is quite similar for both compounds, which can be observed in Figure 5. Nevertheless, when comparing the coupling parameter $\bar{C}$ for both glassy crystals, their behavior is quite disparate. This experimental fact evidences that for temperatures below the plateau, the scattering from low-energy excitations is much weaker for F-113 than for F-112. Even more, when comparing these $\bar{C}$ values to those previously obtained in glassy crystals such as cyclohexanol (4.6×10^{-4}), cyanocyclohexane (4.8×10^{-4}), or ethanol (8.8×10^{-4} for its glassy crystal), it is unquestioned that the $\bar{C}$ value for F-113 clearly appears as the lowest one. The same conclusion can be achieved when compared with some structural glasses such as 2-propanol (5.4×10^{-4}), 1-propanol (3.1×10^{-4}), or ethanol (8.8×10^{-4} for its structural glass).[17,39]

To account for a better description of the thermal conductivity at temperatures higher than $k_B T > W$, we will consider an additional phonon-scattering process which becomes thermally activated at those temperatures, corresponding to resonant scattering of phonons by single oscillators. Such additional contribution was already suggested for F-112 and is described by[17]

$$\tau_{res}^{-1}(\omega, T) = \frac{F\omega^2 T^n}{\left[1 - \frac{\omega^2}{\omega_0^2}\right]^2 + \gamma\left[\frac{\omega}{\omega_0^2}\right]^4}, \qquad (6)$$

where ω_0 is the oscillators' average frequency.

The solid lines in Figure 5 show the thermal conductivity fits using Equation (3) with a relaxation rate $\tau_R^{-1}(x)$ that takes into account the contributions mentioned in Equation (4)

TABLE III. Fit parameters for F-112 and F-113 of the resonant scattering contribution by single oscillators, corresponding to Equation (6). F-113 values are from this work, and F-112 values are from Ref. 17.

Glassy crystal	$\hbar\omega/k_B$ (K)	γ	F (s K^{-2})	n
F-112	25	0.001	5.5×10^{-17}	2
F-113	15	0.001	1.2×10^{-17}	2

and the additional relaxation term for resonant scattering of phonons given by Equation (6). It can be seen that combining the SPM terms and the latter contribution to the phonon relaxation rate, one is able to fully account for the thermal conductivity curves from the lowest temperatures up to the wide plateau. Table III displays the values obtained from the fit for these resonant-scattering contributions, and it evidences that they are much larger for F-112 than for F-113, as the extension of the plateau is larger for the former than for the latter. The most significant differences in behavior of the two compounds concern the large difference in the value of the $\bar{C}$ coupling strength, as well as those for the F and ω_0 parameters within Equation (6). Additional data at hand such as the spectral frequency distributions, recently measured by neutron scattering, are fully consistent with specific heat data as plotted as $C_p \propto T^3$, and therefore cannot explain such large differences. On the other hand, diffraction measurements do not show any striking difference in the disorder of both materials. Thus, the present results call for further detailed studies on the coupling of the lowest internal molecular vibrations to the acoustic field. The expectation is that such torsional vibrations, which in the gas phase have energies within 80 K–250 K (relatively recent accurate measurements for F-113 are given by Le Bris *et al.* in Ref. 30), should be strongly hybridized with the acoustic phonon branches, hence causing these to have a mixed translation/rotation character down to frequencies characteristic of heat transport processes (i.e., within the GHz range). This would mean that any heat-carrying phonon will be strongly coupled to such internal molecular degrees of freedom.

Thermal conductivity for both F-112 and F-113 also experiences pronounced changes at 60 K and 20 K, respectively. This clear kink in the thermal conductivity of F-113 at 20 K as well as the significant change of slope shown by F-112 at 60 K may also be thought of as resulting from anharmonic Umklapp scattering, which is known to dominate the conductivity of insulating crystals at high temperatures. For well ordered crystals (i.e., with low defect concentrations), it leads to a conductivity which decreases with increasing temperature as T^{-1}. There is, however, a caveat for such an assignment, and it concerns how such phonon scattering term can be evaluated from simple models. The latter usually leads to closed form expressions for the Umklapp relaxation rate τ_U^{-1}, which is given in terms of crystal parameters such as the crystal molar volume, Debye frequency, shear modulus, or Grüneisen constant. No conclusive statement can be made because data for the shear moduli and Grüneisen parameters of the two materials are lacking. However, the close values for the molar volume and Debye constant (temperature) of the two materials (see Table I) imply that such models would require the elastic and anharmonic parameters of the two compounds to significantly differ in order to be reconciled with experimental data.

Above these temperatures, the resonant scattering mechanism mentioned above is no longer dominant. Hence, to account for $\kappa(T)$ up to the main glass transition temperatures, we resort to the fact that the materials under scrutiny are in fact translationally ordered solids. In the high temperature region, when both the diffusive and hopping mechanisms are operative, glassy crystals can also experience the effect of the phonon-phonon scattering, which is typical of orientationally ordered crystals above the temperature where the maximum in the phonon thermal conductivity arises. In general, the thermal conductivity of a dielectric crystal can be written as the sum of two contributions,[56] $\kappa(T) = \kappa_1(T) + \kappa_2(T)$, one due to phonons propagating with a mean-free path larger than the phonon half-wavelength, and the other attributed to localized or diffusive short-wavelength vibrational modes. Within this framework, the thermal conductivity can be approximated to a good accuracy by the expression

$$\kappa(T) = \frac{A}{T} + B, \tag{7}$$

where the term A/T comprises the three-phonon Umklapp processes and the term B accounts for the additional mechanism of heat transfer that operates within the high-temperature region. Currently, there is no established theory incorporating both heat transfer mechanisms. However, it is found empirically that, at sufficiently high temperatures, B can be taken as constant.[57] Table IV shows the parameter values resulting from using Equation (7) to fit the thermal conductivity measurements, together with the temperature ranges that have been used. It can be seen that Equation (7) satisfactorily describes the thermal conductivity in the corresponding temperature range. Such a clear T^{-1} dependence shows that the Umklapp process, which is essentially anharmonic phonon-phonon scattering, is dominant in that temperature range.

As far as the values are concerned, the A parameter for F-113 is slightly smaller than for F-112, which would suggest an increase of phonon scattering due to an increase of some disorder in that temperature range. On the other hand, it can be noticed that the additional terms B are smaller than the values found for orientationally ordered molecular crystals.[39,58,59]

An additional striking difference in the behavior of the thermal conductivity of these two materials concerns how this magnitude changes at both sides of the glass-transition temperatures. Data for F-113 display a well defined minimum at such temperature whereas those for F-112 do not show any well defined feature. The absence of a well defined feature at T_g appears to be common to a number of

TABLE IV. Fit parameters for the higher temperature range of the thermal conductivity, corresponding to Equation (7).

Glassy crystal	T (K)	A (W m^{-1})	B (W m^{-1} K^{-1})
F-112	60-90	7.8	0.02
F-113	20-70	5.0	0.085

molecular materials such as those plotted in Figure 6, but contrasts with data for others such as cyclohexanol, which shows more marked changes.[60] Nevertheless, the situation in cyclohexanol may be influenced by the fact that a few kelvin above the glass transition of its plastic crystal, cyclohexanol transforms into another crystalline phase. Moreover, the weak maximum in the thermal conductivity at the glass transition has been argued to be an artifact of the hot-wire method. In any case, the reasons behind such disparate behaviors are difficult to guess because a realistic theory for heat transport in molecular solids is not available, especially for high temperatures where, as epitomized by Equation (7), both phonon-assisted and diffusive heat transport mechanisms are effective. Notice that the underlying assumption for the use of such an equation considers the diffusive contribution to be a constant at high temperatures within the dynamically arrested phase, and also that an additional heat transport channel should become operative above T_g arising from the quasi-free molecular rotations. The current results thus call for additional research on these topics. Molecular simulations of heat-transport phenomena on these materials may be of help to separate the different transport mechanisms here in operation.

V. SUMMARY AND CONCLUSIONS

We have measured the specific volume, thermal conductivity, and specific heat of the glassy crystals of 1,2,2-trichloro-1,1,2-trifluoroethane (CCl_2F–$CClF_2$, F-113) and 1,1,2,2-tetrachloro-1,2-difluoroethane (CCl_2F–CCl_2F, F-112) from 1.7 K up to their plastic crystal phases, and well above the corresponding glass transition temperatures. Measurements of these crystals display a rich behavior. In this work we have focused on the discussion of the F-113 features at 20, 72, and 120 K. Several anomalies have been rationalized in terms of degrees of freedom that become arrested, such as the internal molecular rotation, which undergoes a conformational arrest (T_a = 120 K), and the overall molecular rotation, which freezes at the main glass transition (T_g = 72 K for F-113). These features have been compared to those of F-112, which has its counterparts at 60, 89.5, and 130 K, respectively.

The specific heat and the thermal conductivity at the lowest temperatures can be both understood by recourse to the SPM which needs to be supplemented with an additional phonon-scattering contribution, ascribed to resonant scattering of phonons by single oscillators.

In stark contrast to structural glasses and other glassy crystals, the plateau exhibited by the thermal conductivity is followed by a kink and a further *decrease* in conductivity with increasing temperature up to the temperatures signaling a glass-transition. Such behavior is here attributed to a high density of thermally activated degrees of freedom due to the interplay of orientational and internal molecular low-energy motions.

The study here reported on materials exhibiting internal molecular rotational isomerism comes into line with previous studies on the structural and thermodynamic properties of materials composed by chemical isomers which have shown how a minor chemical modification can lead to strikingly disparate behaviors.[61–64] The results thus call for a re-examination of some current assumptions pertaining the universality of properties exhibited by disordered matter.

ACKNOWLEDGMENTS

This work was financially supported in part by the Spanish Ministry of Science and Innovation (Grant Nos. FIS2014-54734-P, FIS2011-23488, and MAT2014-57866-REDT), by the Catalan Government (Grant No. 2014SGR-0581) and by the Comunidad de Madrid through program NANOFRONTMAG-CM (No. S2013/MIT-2850), as well as by the joint NAS Ukraine and Russian Foundation for Basic Research project "Metastable states of simple condensed systems" (Agreement No. N 7/-2013).

[1]J. Timmermans, J. Phys. Chem. Solids **18**, 1 (1961).
[2]*The Plastically Crystalline State: Orientationally Disordered Crystals*, edited by J. N. Sherwood (John Wiley & Sons, New York, 1978).
[3]H. Suga and S. Seki, J. Non-Cryst. Solids **16**, 171 (1974).
[4]R. W. Cahn, Nature **253**, 310 (1975).
[5]E. K. Plyler, J. Chem. Phys. **17**, 218 (1949).
[6]R. E. Kagarise and D. H. Rank, Trans. Faraday Soc. **48**, 394 (1952).
[7]K. Naito, I. Nakagawa, K. Kuratani, I. Ichishima, and S. Mizushima, J. Chem. Phys. **23**, 1907 (1955).
[8]J. P. Zietlow, F. F. Cleveland, and A. G. Meister, J. Chem. Phys. **24**, 142 (1956).
[9]R. E. Kagarise, J. Chem. Phys. **24**, 300 (1956).
[10]M. Takeda and H. S. Gutowsky, J. Chem. Phys. **26**, 577 (1957).
[11]J. W. Brasch, J. Chem. Phys. **43**, 3473 (1965).
[12]V. P. Kolesov, E. A. Kosarukina, D. Yu. Zhogin, M. E. Poloznikova, and Yu. A. Pentin, J. Chem. Thermodyn. **13**, 115 (1981).
[13]V. Kolesov, Thermochim. Acta **266**, 129 (1995).
[14]L. C. Pardo, P. Lunkenheimer, and A. Loidl, J. Chem. Phys. **124**, 124911 (2006).
[15]M. Rovira-Esteva, N. A. Murugan, L. C. Pardo, S. Busch, J. Ll. Tamarit, Sz. Pothoczki, G. J. Cuello, and F. J. Bermejo, Phys. Rev. B **84**, 064202 (2011).
[16]K. Kishimoto, H. Suga, and S. Seki, Bull. Chem. Soc. Jpn. **51**, 1691 (1978).
[17]I. V. Sharapova, A. I. Krivchikov, O. A. Korolyuk, A. Jezowski, M. Rovira-Esteva, J. Ll. Tamarit, L. C. Pardo, M. D. Ruiz-Martin, and F. J. Bermejo, Phys. Rev. B **81**, 094205 (2010).
[18]L. C. Pardo, F. J. Bermejo, J. Ll. Tamarit, G. J. Cuello, P. Lunkenheimer, and A. Loidl, J. Non-Cryst. Solids **353**, 999 (2007).
[19]M. Rovira-Esteva, L. C. Pardo, J. Ll. Tamarit, and F. J. Bermejo, in *Metastable Systems under Pressure*, NATO Science for Peace and Security Series: A. Chemistry and Biology, edited by S. J. Rzoska, A. Drozd-Rzoska, and V. Mazur (Springer, Netherlands, 2009), pp. 63–77.
[20]Ph. Negrier, M. Barrio, J. Ll. Tamarit, L. C. Pardo, and D. Mondieig, Cryst. Growth Des. **12**, 1513 (2012).
[21]Ph. Negrier, J. Ll. Tamarit, M. Barrio, and D. Mondieig, Cryst. Growth Des. **13**, 782 (2013).
[22]Ph. Negrier, M. Barrio, J. Ll. Tamarit, D. Mondieig, M. J. Zuriaga, and S. C. Perez, Cryst. Growth Des. **13**, 2143 (2013).
[23]S. Wolfe, Acc. Chem. Res. **5**, 102 (1972).
[24]R. C. Bingham, J. Am. Chem. Soc. **98**, 535 (1976).
[25]R. J. Abraham and K. Parry, J. Chem. Soc. B **1970**, 539.
[26]J. R. Durig, J. Liu, T. S. Little, and V. F. Kalasinsky, J. Phys. Chem. **96**, 8224 (1992).
[27]R. A. Newmark and C. H. Sederhol, J. Chem. Phys. **43**, 602 (1965).
[28]R. A. Newmark and R. E. Graves, J. Phys. Chem. **72**, 4299 (1968).
[29]R. A. Pethrick and E. Wyn-Jones, J. Chem. Soc. A **1971**, 54.
[30]K. L. Bris, K. Strong, S. M. L. Melo, and J. C. Ng, J. Mol. Spectrosc. **243**, 142 (2007).
[31]M. Iwasaki, Bull. Chem. Soc. Jpn. **32**, 205 (1959).
[32]H. Hallam and T. Ray, J. Mol. Spectrosc. **12**, 69 (1964).
[33]H.-N. Lee, L.-C. Chang, and T.-M. Su, Chem. Phys. Lett. **507**, 63 (2011).
[34]E. Pérez-Enciso and M. A. Ramos, Thermochim. Acta **461**, 50 (2007).
[35]M. Hassaine, R. J. Jiménez-Riobóo, I. V. Sharapova, O. A. Korolyuk, A. I. Krivchikov, and M. A. Ramos, J. Chem. Phys. **131**, 174508 (2009).
[36]T. Pérez-Castañeda, J. Azpeitia, J. Hanko, A. Fente, H. Suderow, and M. A. Ramos, J. Low Temp. Phys. **173**, 4 (2013).

[37]A. I. Krivchikov, V. G. Manzhelii, O. A. Korolyuk, B. Ya. Gorodilov, and O. O. Romantsova, Phys. Chem. Chem. Phys. **7**, 728 (2005).
[38]A. I. Krivchikov, B. Ya. Gorodilov, and O. A. Korolyuk, Instrum. Exp. Tech. **48**, 417 (2005).
[39]A. I. Krivchikov, O. A. Korolyuk, I. V. Sharapova, J. Ll. Tamarit, F. J. Bermejo, L. C. Pardo, M. Rovira-Esteva, M. D. Ruiz-Martin, A. Jezowski, J. Baran, and N. A. Davydova, Phys. Rev. B **85**, 014206 (2012).
[40]A. I. Krivchikov, M. Hassaine, I. V. Sharapova, O. A. Korolyuk, R. J. Jiménez-Riobóo, and M. A. Ramos, J. Non-Cryst. Solids **357**, 524 (2011).
[41]M. Hassaine, M. A. Ramos, A. I. Krivchikov, I. V. Sharapova, O. A. Korolyuk, and R. J. Jiménez-Riobóo, Phys. Rev. B **85**, 104206 (2012).
[42]J. K. Krüger, J. Schreiber, R. Jimenez, K.-P. Bohn, F. Smutny, M. Kubat, J. Petzelt, J. Hrabovska-Bradshaw, S. Kamba, and J. F. Legrand, J. Phys.: Condens. Matter **6**, 6947 (1994).
[43]*Amorphous Solids: Low Temperature Properties*, edited by W. A. Phillips (Springer, Berlin, 1981).
[44]M. A. Ramos, S. Vieira, F. J. Bermejo, J. Dawidowski, H. E. Fischer, H. Schober, M. A. González, C. K. Loong, and D. L. Price, Phys. Rev. Lett. **78**, 82 (1997).
[45]A. I. Krivchikov, A. N. Yushchenko, V. G. Manzhelii, O. A. Korolyuk, F. J. Bermejo, R. Fernández-Perea, C. Cabrillo, and M. A. González, Phys. Rev. B **74**, 060201(R) (2006).
[46]V. A. Konstantinov, A. I. Krivchikov, O. A. Korolyuk, V. P. Revyakin, V. V. Sagan, G. A. Vdovichenko, and A. V. Zvonaryova, Phys. B **424**, 54 (2013).
[47]R. C. Zeller and R. O. Pohl, Phys. Rev. B **4**, 2029 (1971).
[48]U. Buchenau, Yu. M. Galperin, V. L. Gurevich, D. A. Parshin, M. A. Ramos, and H. R. Schober, Phys. Rev. B **46**, 2798 (1992).
[49]M. A. Ramos and U. Buchenau, Phys. Rev. B **55**, 5749 (1997).
[50]M. A. Ramos and U. Buchenau, in *Tunneling Systems in Amorphous and Crystalline Solids*, edited by P. Esquinazi (Springer, Berlin, 1998), p. 527.
[51]E. Bonjour, R. Calemczuk, R. Lagnier, and B. Salce, J. Phys. (Paris) **42**, 63 (1981).
[52]D. A. Parshin, Phys. Rev. B **49**, 9400 (1994).
[53]M. A. Ramos, Philos. Mag. **84**, 1313 (2004).
[54]J. K. Krüger, J. Baller, T. Britz, A. le Coutre, R. Peter, R. Bactavatchalou, and J. Schreiber, Phys. Rev. B **66**, 012206 (2002).
[55]J. J. Freeman and A. C. Anderson, Phys. Rev. B **34**, 5684 (1986).
[56]A. I. Krivchikov, O. A. Korolyuk, and I. V. Sharapova, Low Temp. Phys. **38**, 74 (2012), and references therein.
[57]J. L. Feldman, M. D. Kluge, P. B. Allen, and F. Wooten, Phys. Rev. B **48**, 12589 (1993).
[58]A. I. Krivchikov, I. V. Sharapova, O. A. Korolyuk, O. O. Romantsova, and F. J. Bermejo, Low Temp. Phys. **35**, 891 (2009).
[59]O. A. Korolyuk, Low Temp. Phys. **37**, 416 (2011).
[60]O. Andersson, R. G. Ross, and G. Bäckström, Mol. Phys. **66**, 619 (1989).
[61]C. Talón, F. J. Bermejo, C. Cabrillo, G. J. Cuello, M. A. González, J. W. Richardson, A. Criado, M. A. Ramos, S. Vieira, F. L. Cumbrera, and L. M. González, Phys. Rev. Lett. **88**, 115506 (2002).
[62]C. Talón, M. A. Ramos, S. Vieira, I. M. Shmyt'ko, N. Afonikova, A. Criado, G. Madariaga, and F. J. Bermejo, J. Non-Cryst. Solids **287**, 226 (2001).
[63]M. A. Ramos, M. Hassaine, B. Kabtoul, R. J. Jiménez-Riobóo, I. M. Shmyt'ko, A. I. Krivchikov, I. V. Sharapova, and O. A. Korolyuk, Low Temp. Phys. **39**, 468 (2013).
[64]R. Böhmer, C. Gainaru, and R. Richert, Phys. Rep. **545**, 125 (2014).